SUPPORTING INFORMATION

Metal Ion Binding at the Catalytic Site Induces Widely Distributed Changes in a Sequence Specific Protein-DNA Complex

Kaustubh Sinha[1,2], Sahil S. Sangani[2], Andrew D. Kehr[2]

Gordon S. Rule[2,*] and Linda Jen-Jacobson[1,*]

[1] Department of Biological Sciences, University of Pittsburgh, Pittsburgh PA 15260 USA

[2] Department of Biological Sciences, Carnegie Mellon University, Pittsburgh PA 15213 USA

Supplementary Tables

Table S1. Sidechain truncation mutations cause CSPs

Mutation	Prominent Methyl CSPs No Lu^{3+}	Prominent Methyl CSPs +Lu^{3+}
Isoleucines		
I23V	I43	I43
I30V	I24, I159	I24, I159
I43V	ND	I51
I51V	I43, I55	I43, I52, I55
I52V	I43, I55, I91, I134	I24, I30, I43, I91, I133
I89V	I51, I52, I55, I91	I52, I55, I91
I91V	I52, I134	I52, I134
I133V	I43, I51, I91	I52
Valines		
V20A	I43, I51 (no CSP in LV peaks)	I24, I30, I43*,I52, I91 L3δ1, L33δ2, V63γ1, L156δ1, V166γ2, V168γ2
V63A	I24, I30, I43, I51, I52, I55, I91, I133, I134 L3δ2, L7δ2, L77δ1, L148δ1, V166γ1γ2, V168γ1γ2	I24, I30, I51, I52, I91, L3δ1, L77δ2, L148δ1, V166γ1γ2, V168γ1γ2
Leucines		
L156V	I24, I30, I43, I153 (no CSP LV peaks)	I24, I30, I153, V122γ1

*Spot intensifies but does not shift
Other mutants examined are listed in Materials & Methods.

Table S2. Crystallographic data collection and refinement statistics for EcoRV-DNA-Lu^{3+} complexes

	5F8A Intact DNA	5HLK Cleaved DNA
Data collection		
Space group	P1	P1
Cell dimensions		
a, b, c (Å)	46.43, 52.86, 65.31	47.62, 48.33, 63.53
α, β, γ (°)	70.61, 73.24, 81.81	96.94, 108.78, 106.70
Resolution range (Å)	24.90-1.76 (1.85-1.76)	38.11-2.00 (2.05-2.00)
Wavelength (Å)	1.54178	1.54178
R_{sym} or R_{merge}	0.051 (0.196)	0.051 (0.224)
I / σI	14.7 (4.4)	20.3 (3.2)
Completeness (%)	93.0 (88.9)	84.3 (27.8)
Redundancy	3.9 (3.2)	4.3 (1.7)
Refinement		
Resolution (Å)	1.76	2.00
No. reflections	46648	26617
R_{work} / R_{free}	0.159 / 0.202	0.165 / 0.228
R_{free} test set	10.71%	5.13%
B-factors		
Wilson plot ($Å^2$)	21.69	18.60
Overall ($Å^2$)	27.61	22.44
Ramachandran plot		
Favored	464 (97.3%)	463 (96.3%)
Outliers	4 (0.84%)	3 (0.62%)
R.m.s. deviations		
Bond lengths (Å)	0.017	0.016
Bond angles (°)	1.876	1.780

Values in parentheses are for highest-resolution shell.

Table S3: Conformational analysis of DNA in crystal structures of EcoRV-DNA complexes [a]

PDB entry	Space group	Metal ion	DNA sequence [c,d]	Overall Bend [e]	Roll angle at TA step	Minor groove width (Å) at TA step
5F8A	P1	Lu^{3+}	AAAGATATCTTT	55.5°	55.5°	10.6
1B95	P1	None	AAAGATATCTT	42.9°	53.6°	10.5
1B94	P1	Ca^{2+}	AAAGATATCTT	43.4°	57.1°	10.4
4RVE (I)[b]	$C222_1$	None	GGGATATCCC	49.1°	44.4°	11.7
1EOO (II)	$C222_1$	None	GAAGATATCTTC	59.1°	49.1°	10.3
1RVA (III)	P1	None	AAAGATATCTT	42.7°	47.3°	10.2
1EOP (IV)	$P4_12_12$	None	AAGATATCTTA	44.2°	36.6°	10.2
1RVB	P1	Mg^{2+}	AAAGATATCTT	43.1°	54.4°	10.2
1RVC	P1	Mg^{2+}	AAAGAT|ATCTT	44.1°	35.7°	7.7
5HLK	P1	Lu^{3+}	AAAGAT|ATCTTT	38.3°	54°	8.0

[a] DNA structural parameters calculated with Curves+ program provided by Lavery et al. [1]
[b] Crystal lattice forms (I –IV) designated by Horton and Perona [2].
[c] Bases used to define the best-fit curvilinear axis are underlined.
[d] Vertical bar at TA step indicates cleaved DNA.
[e] Overall bend of helix axis calculated using a best-fit curvilinear axis to underlined bases.

Supplementary Figures

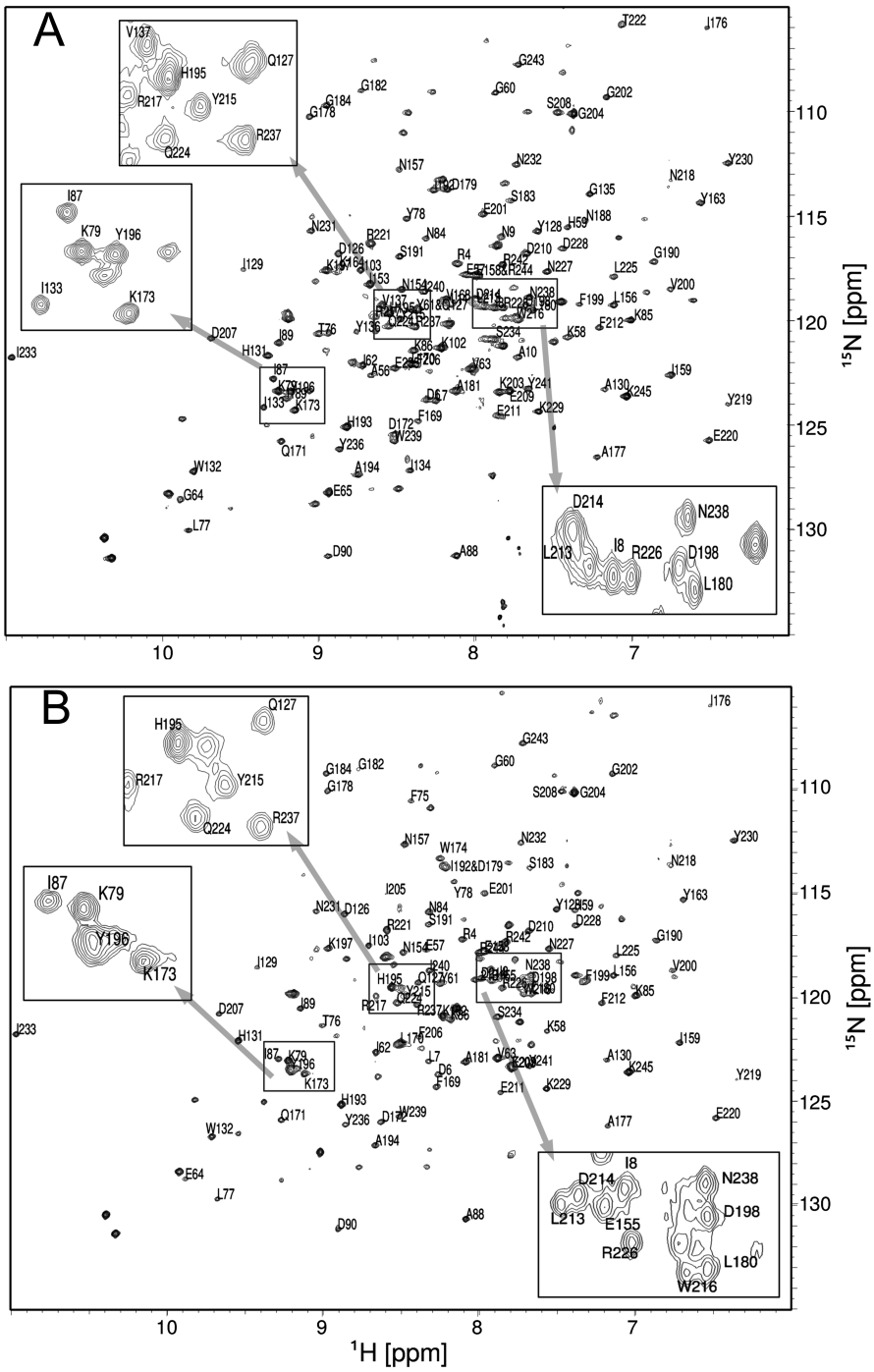

Figure S1. **Peak assignments in the two dimensional ^{1}H–^{15}N correlation spectra (TROSY) of the EcoRV-DNA complexes.** Assignments were based on inter-residue chemical shifts involving C_α, C_β, and carbonyl carbon shifts, distance information from amide-amide NOEs, and carbonyl specifically labeled samples. A number of amide resonances are not observable, possibly due to dipolar interactions with the protonated DNA. Although the majority of observed resonances are assigned, a small number of peaks remained unassigned due to missing connectivities to other residues. Spectra of metal-free complex (A) and complex with saturating Lu^{3+} (B).

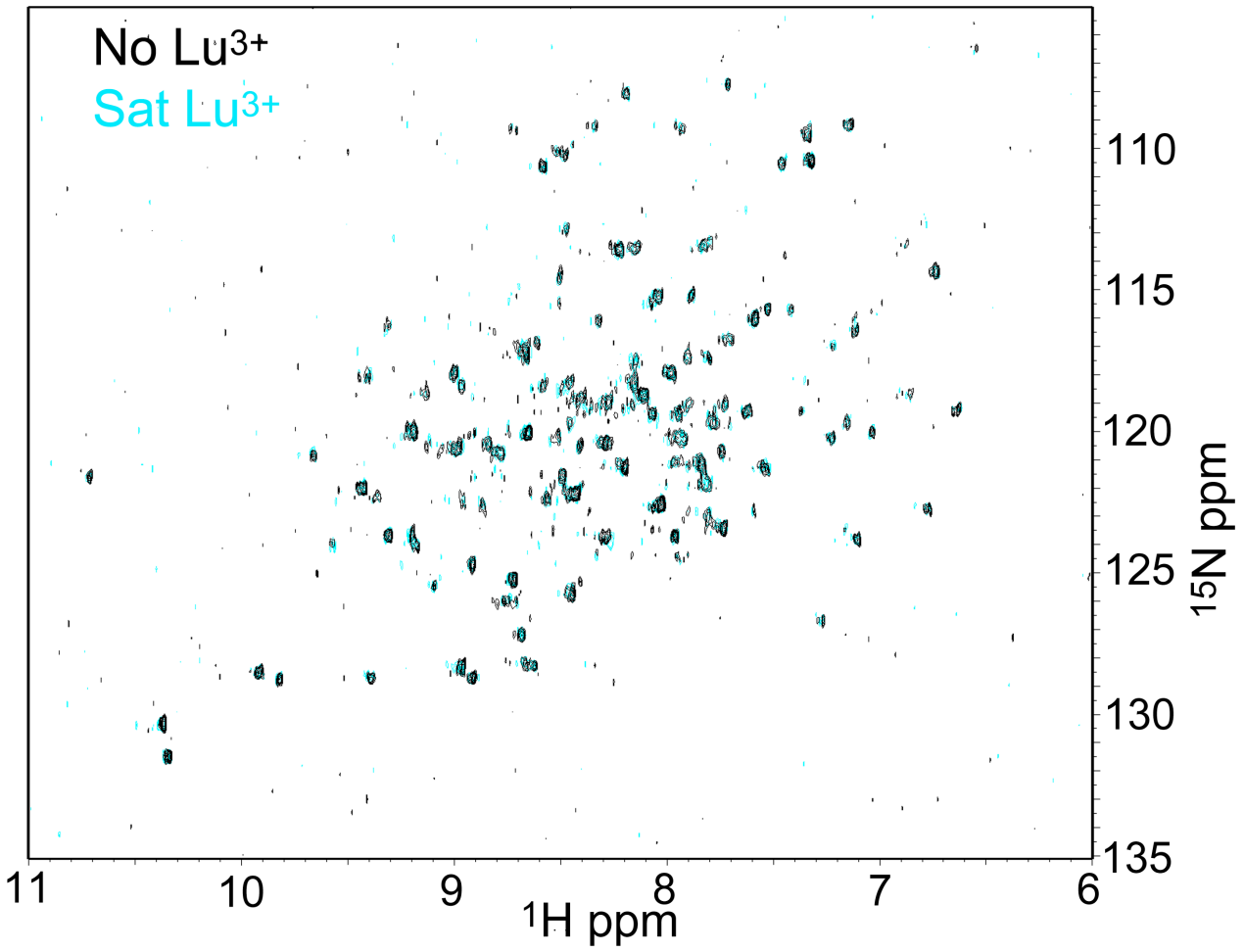

Figure S2. ^{1}H-^{15}N HSQC-TROSY spectra of nonspecific EcoRV-DNA complexes. Black peaks indicate no metal ions and cyan peaks indicate saturating Lu^{3+}. The near-complete absence of CSPs indicates that metal-ion binding sites are not assembled in the nonspecific EcoRV-DNA complex, consistent with the methyl resonance data in Figures 1D and 1F.

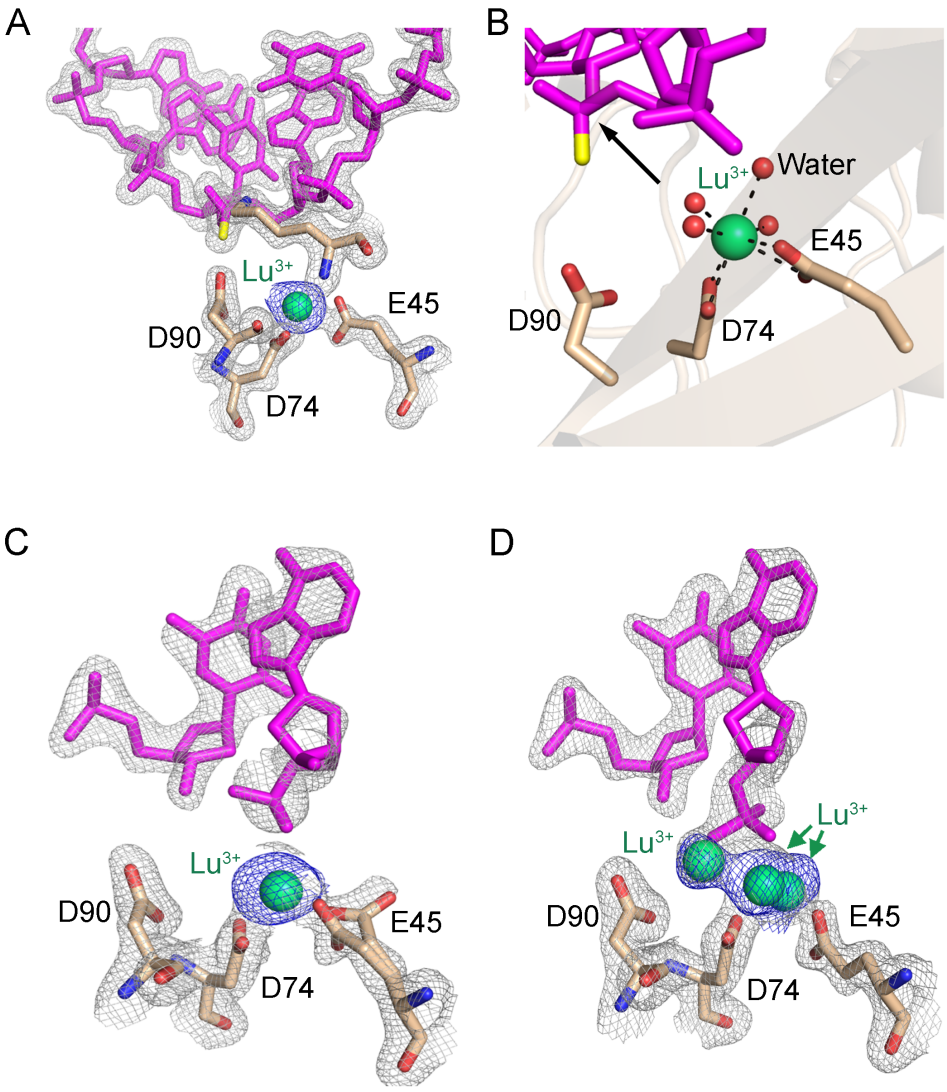

Figure S3. Lu^{3+} coordination in EcoRV-DNA-Lu3+ complexes with uncleaved and cleaved DNA. DNA is colored magenta, residues from EcoRV are CPK (carbon light brown), and Lu^{3+} ions are teal. $2F_o$-F_C maps are gray and contoured at 2σ (A) or 1σ (C and D). Anomalous difference maps are blue and contoured at 5σ (A) or 3σ (C and D). Panels (A) and (B) show the complex with uncleaved DNA (PDB entry 5F8A), with active site sidechains (E45, D74, D90) labeled. The Lu^{3+} ion is in neither the A-site nor the B-site occupied by Mg^{2+} in PDB entry 1RVB. Panel (B) shows the octahedral coordination sphere for Lu^{3+}, with ligands within 2.6 Å of the Lu^{3+} ion. Arrow indicates the scissile phosphate. Panels (C) and (D) show bound Lu^{3+} in the two different active sites of the post-cleavage complex (PDB entry 5HKL). K92 and additional DNA bases were removed for clarity.

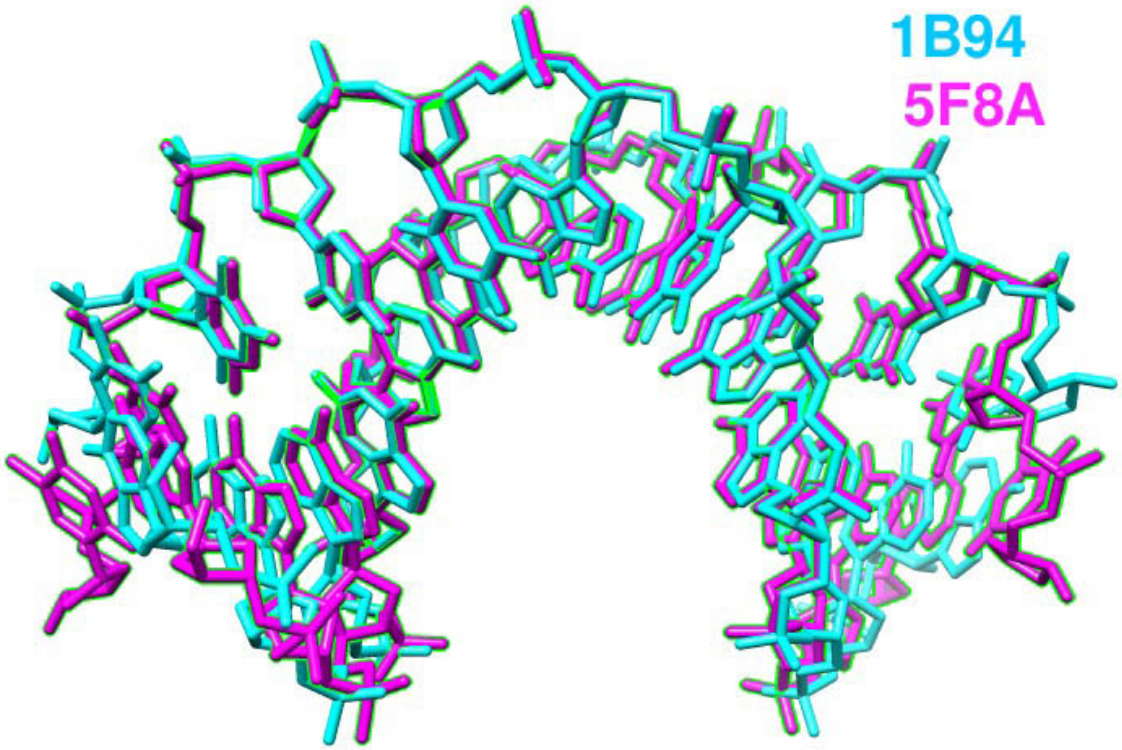

Figure S4. Comparison of DNA bends in EcoRV-DNA crystal structures with 2 Lu^{3+} (PDB entry 5F8A, magenta) or 2 Ca^{2+} (PDB entry 1B94, cyan). Models were aligned on the backbones of EcoRV residues 62-93 (includes strands ß1, ß2, ß3; cf. Fig. 5). Detailed conformational parameters are given in Table S3.

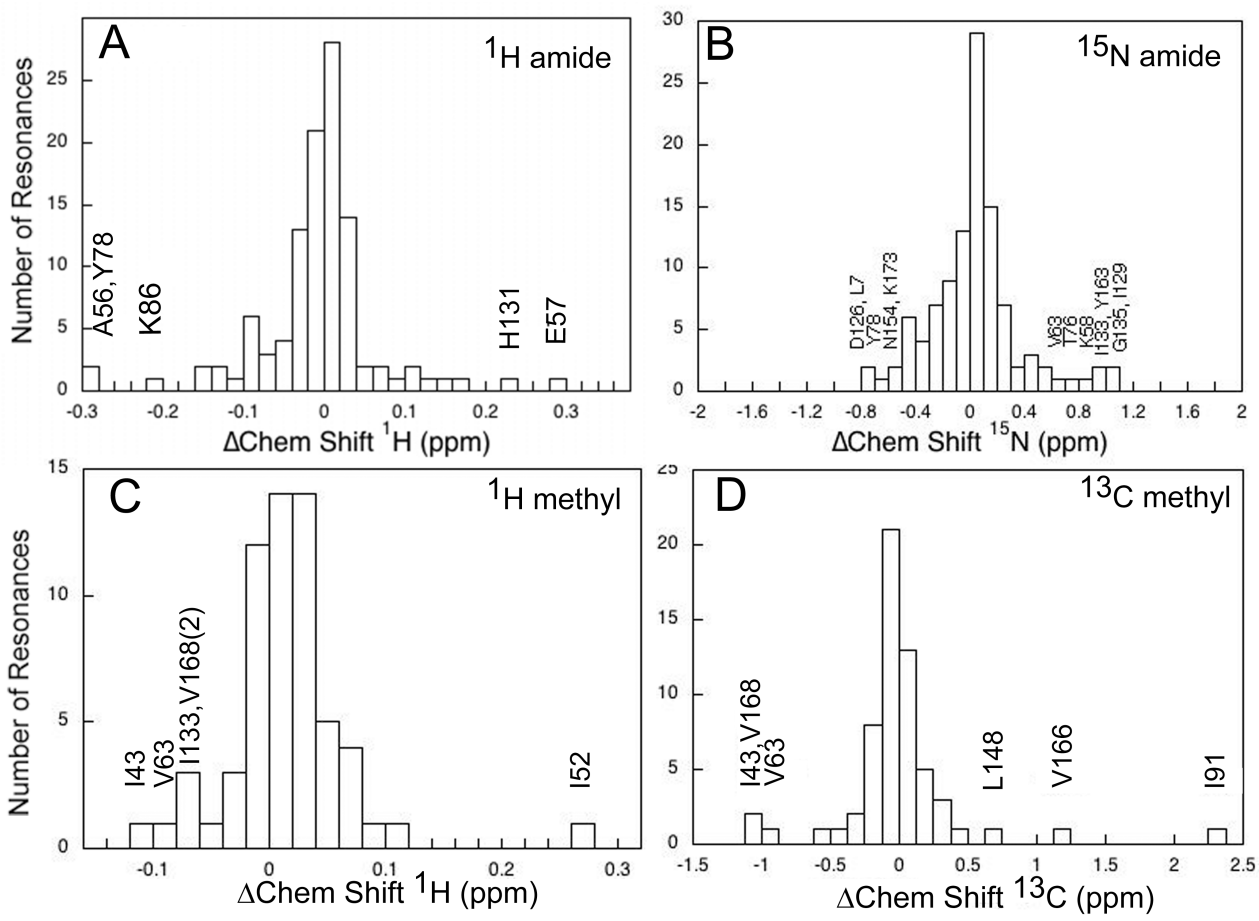

Figure S5. Distributions of (A and B) amide (^{1}H and ^{15}N) and (C,D) methyl (^{1}H and ^{13}C) chemical shift changes induced by saturating Lu^{3+}. In all cases, the X-axis shows the chemical shift in the designated EcoRV-DNA-$(Lu^{3+})_4$ complex minus that in the EcoRV-DNA complex with no metal. Residues with unusually large $\Delta\delta$ are labeled above the appropriate bars.

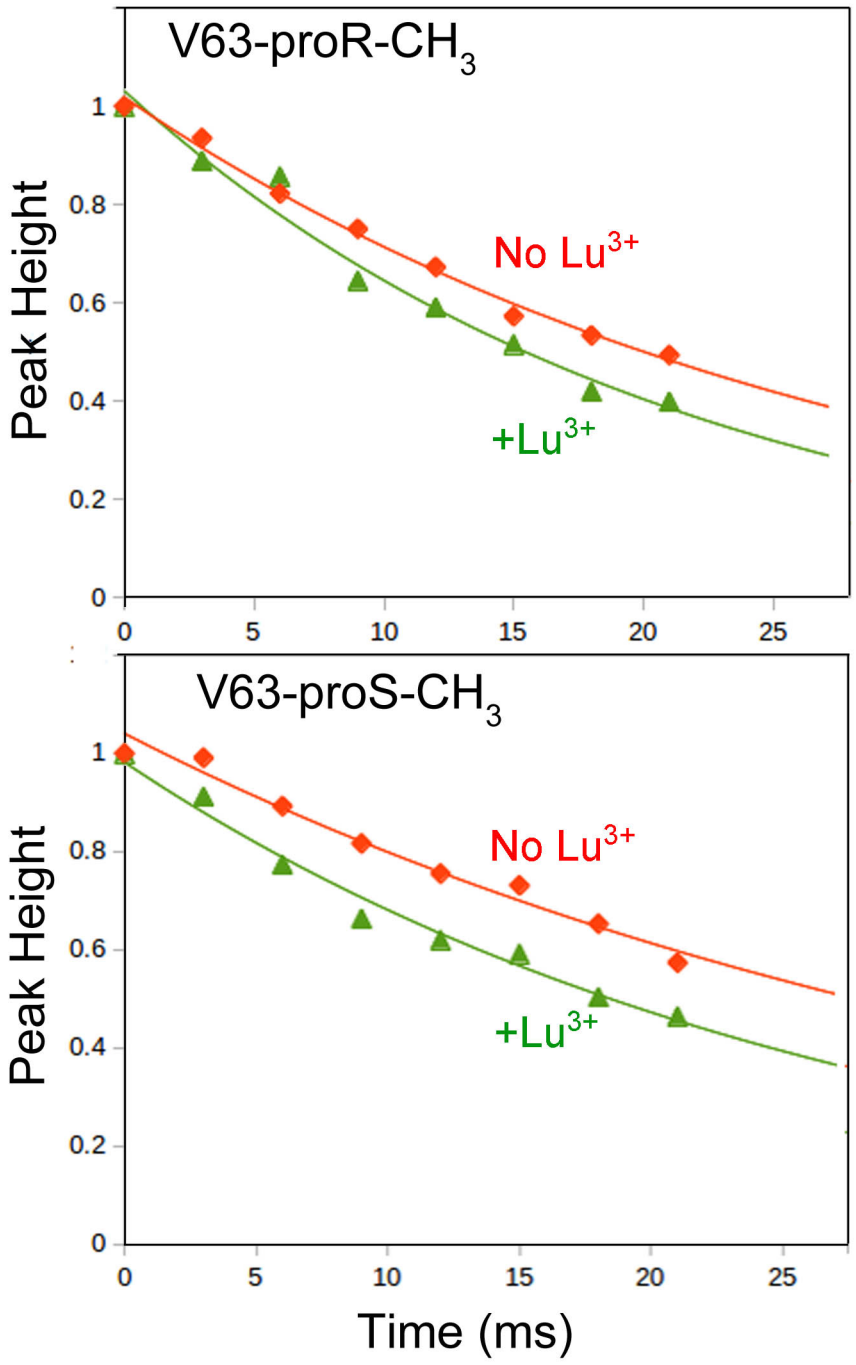

Figure S6. ^{1}H transverse relaxation decay curves of stereospecifically assigned V63 methyl side-chain in EcoRV-DNA and EcoRV-DNA-$(Lu^{3+})_4$ complexes. This complex was labeled with diamagnetic MTS (Materials and Methods) at position S234C, as a control in a series of PRE studies. Experimental data were fitted to a two-parameter single exponential function to obtain relaxation rate constants as follows. proR-CH_3 no Lu^{3+}: 0.035±0.001 s^{-1}; proR-CH_3 + Lu^{3+}: 0.046±0.003 s^{-1}; proS-CH_3 no Lu^{3+}: 0.026±0.002 s^{-1}; proR-CH_3 + Lu^{3+}: 0.038±0.002 s^{-1}.

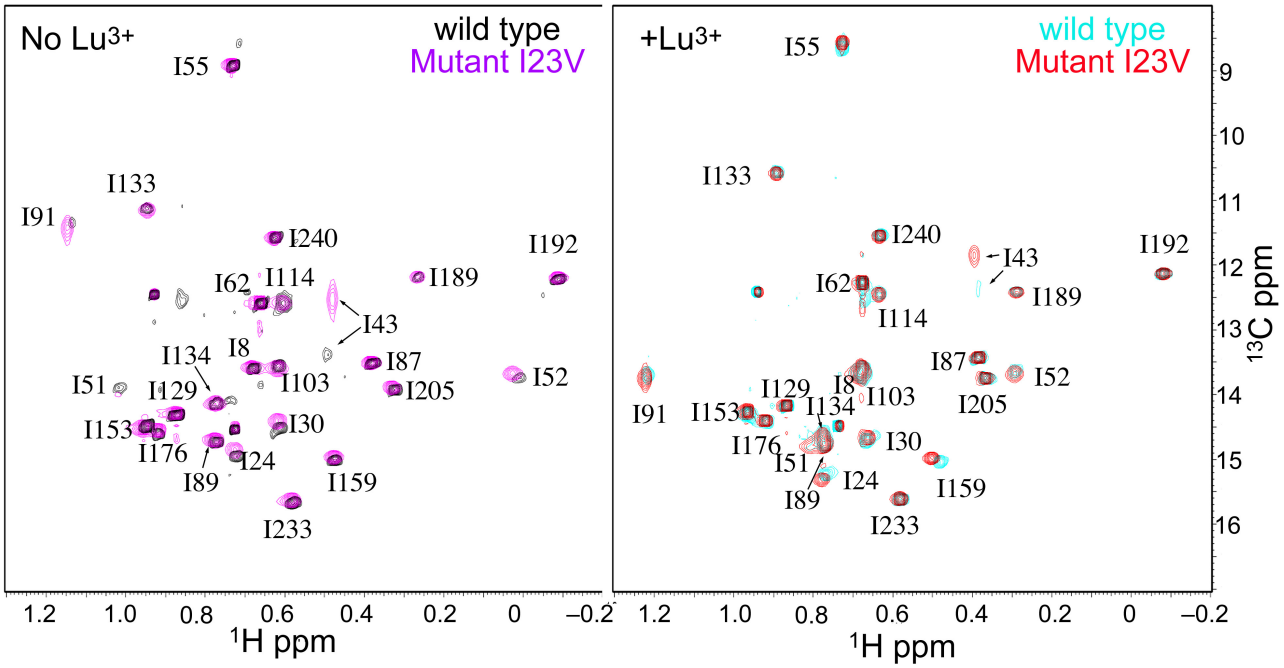

Figure S7. Effect of the I23V mutation on Ile-δ-CH_3 resonances with and without saturating Lu^{3+}. The mutation primarily affects the peak for I43-δ-CH_3 (see Discussion). The resonance for I23-δ-CH_3 itself is unassigned.

References

(1) Lavery, R., Moakher, M., Maddocks, J. H., Petkeviciute, D., and Zakrzewska, K. (2009) Conformational analysis of nucleic acids revisited: Curves, *Nucleic Acids Research 37*, 5917-5929.

(2) Horton, N. C., and Perona, J. J. (2000) Crystallographic snapshots along a protein-induced DNA-bending pathway, *Proc. Natl. Acad. Sci. U S A 97*, 5729-5734.